Heliyon 10 (2024) e36265

Contents lists available at ScienceDirect

Heliyon

journal homepage: www.cell.com/heliyon

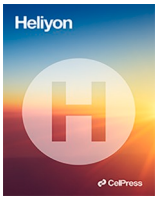

Review article

Mechanical properties of intercellular tunneling nanotubes formed by different mechanisms

Yanli Sun [a], Huikai Zhang [a], Ilya B. Zavodnik [b], Hucheng Zhao [a,*], Xiqiao Feng [a,**]

[a] Institute of Biomechanics and Medical Engineering, Department of Engineering Mechanics, School of Aerospace Engineering, Tsinghua University, Beijing, 100084, China
[b] Department of Biochemistry, Yanka Kupala State University of Grodno, 230030, Grodno, Belarus

ARTICLE INFO

Keywords:
Cell
TNT
Tensile strength
F-actin
Cadherin
Mechanical model

ABSTRACT

Tunneling nanotubes (TNTs) that connect cells have been recognized as a pathway for long-range intercellular transport of diverse cargoes, including viruses, lysosomes or other organelles, Ca^{2+} and electrical signals. TNTs can initially be formed from thin finger-like actin assembly-driven protrusions or cell contacts and dislodgment. However, it remains unclear whether the mechanical properties of TNTs formed by these two mechanisms are the same. Here, we developed novel microoperation methods to investigate the mechanical properties of TNTs in HEK293 cells, in which the TNTs form from thin finger-like actin assembly-driven protrusions and C2C12 cells, in which the TNTs form through contact and cell dislodgment. We found that TNTs formed by the two mechanisms represent elastic elements with similar tensile strength. In both the HEK and C2C12 cells, the tensile strength of TNTs exhibited a distinct size dependence on their lengths and diameters. Disturbing the cytoskeleton or removing extracellular Ca^{2+} also changed their tensile strength. In addition, the stiffening of the extracellular matrix (ECM) enhanced the length, diameter and tensile strength of TNTs both in both HEK and C2C12 cells. Finally, a theoretical model was established to reveal the changes in the TNT's mechanical properties with its length, diameter and individual tunneling nanotubes (iTNT) number. This work not only gains insights into the properties of TNTs but also helps understand the dynamics of various cells.

1. Introduction

Intercellular communication plays a crucial role in numerous physiological processes of multicellular organisms, including the coordination of cellular activities, responses to environmental changes, as well as intricate biological processes such as development, immune responses, and tissue repair [1,2]. In 2004, Rustom et al. discovered TNTs among rat neuronal PC12 cells [3]. Subsequent studies showed that TNT connections exist between various cell types, including immune cells, astrocytes, neurons, and tumor cells. These cells use TNTs to transfer diverse cellular cargos, such as endocytic vesicles, mitochondria, pieces of the endoplasmic reticulum, and cytoplasmic molecules [4–6]. Notably, TNTs can be formed by two different mechanisms. The first mechanism is based on the ability of either one or two of the communicating cells to induce the outgrowth of filopodia-like protrusions, and the elongation of these protrusions is followed by cell-cell contact and membrane fusion [7]. The second mechanism of TNT formation is based on cell

* Corresponding author.
** Corresponding author.
E-mail addresses: zhaohc@mail.tsinghua.edu.cn (H. Zhao), fengxq@tsinghua.edu.cn (X. Feng).

https://doi.org/10.1016/j.heliyon.2024.e36265
Received 22 December 2023; Received in revised form 9 July 2024; Accepted 13 August 2024
Available online 15 August 2024

dislodgment, whereby cells make contact and then form a nanotube when they move apart [7]. Noted that the diameter and length of TNTs formed by these two mechanisms vary significantly. Recent reports indicated that these cell-cell contacts may be made up of several iTNTs in neuronal cells and other cell types [2,8,9]. Despite the heterogeneity in their morphologies and formation mechanisms, TNTs allow for bi- and uni-directional communication by transferring electrical signals, cellular compounds, and vesicles, resulting in so-called intercellular nanotubular highways [3,10]. As TNTs can fracture due to mechanical forces and they are very close to the substrate. TNT-dependent information transfer can be disturbed by mechanical stress [11], which determines the number of TNTs. Recently, some experiments have been conducted to probe the mechanical properties of TNTs, but the current methods based on atomic force microscopy or optical tweezers encounter challenges in the measurement of large TNT deformation [9,12]. In addition, it remains unclear whether the TNTs formed by the two different mechanisms have similar mechanical properties. In this study, we investigated the mechanical properties of TNTs formed using two different mechanisms by more accurate experimental methods, which allowed us to understand the main molecular component determining the mechanical properties of TNTs.

2. Materials and methods

2.1. Preparation of polyacrylamide (PA) gels with a defined stiffness

Polyacrylamide (PA) gels with different stiffness were fabricated by combining specific amounts of acrylamide and bisacrylamide, as described previously [13]. After functionalization with 0.1 mM Sulfo-SANPAH (Thermo Fisher Scientific, USA), the gels were coated with 10 $\mu g/cm^2$ of rat tail collagen type-I (Sigma Aldrich, USA) overnight at 4 °C to obtain a uniform surface coating.

2.2. Cell culture and drug treatment

HEK and C2C12 cells were cultured in DMEM (Corning, USA), complemented with 10 % fetal bovine serum (FBS; Gibco, USA) and 100 U/ml penicillin/streptomycin. The cells were incubated at 37 °C with 5 % CO_2 and 95 % relative humidity. The cells were treated with cytochalasin D (Sigma; 10 μM, 45min) to inhibit the polymerization of F-actin.

2.3. Actin staining

HEK and C2C12 cells were immobilized using 4 % paraformaldehyde (Sigma) and subsequently permeabilized using 0.2 % Triton X-100 (Sigma) for 20 min. A blocking step was then conducted with 5 % bovine serum albumin (BSA, Amresco, USA) for 1.5 h after which the cells were incubated with 1:1000 fluorescently labeled phalloidin conjugated Texas red (AAT; Bioquest, USA). All fluorescence-labeled samples were imaged using a Zeiss 710 confocal microscope equipped with a 40 × /0.75NA objective (Carl Zeiss Microimaging, Japan).

2.4. Immunostaining

For the staining of tubulin in HEK and C2C12 cells, cells were labeled with tubulin ABCAM 179484 antibody (1:200) and Alexa Fluor 594-conjugated secondary antibodies (1:500).

2.5. Micropipette experiment and imaging apparatus

Cells were placed on the stage of an Olympus IX73 inverted microscope equipped with a xenon illumination system and an IMAGO CCD camera (Till Photonics, Germany). Bright-field imaging was performed using a sCMOS camera (PCO. edge, PCO, Germany) with a full-frame sampling interval of 1s corresponding to a camera frame rate of 1 Hz. The midpoint of the TNTs was pushed using the MP-225 Micromanipulator (Sutter Instrument Company, USA) with a fire-polished glass pipette (see the corresponding movies in the Supplementary Movies). The maximum elongation was defined as the ratio of TNT length when pushed with a glass pipette until it ruptured to the initial length of the TNT before pushing.

2.6. Statistical analysis

Each set of experimental data was acquired from three independent experiments and was presented as the mean ± SEM. Two-tailed Student's t-test was employed for analysis of the difference between the two groups, while comparisons involving a minimum of three groups were assessed through analysis of variance (ANOVA). In all instances, statistical significance was determined by a P-value of <0.05. All statistical analyses were performed using GraphPad Prism 9.5.1 software (GraphPad Inc, USA).

3. Results

3.1. Formation and geometric characteristics of TNTs in HEK and C2C12 cells

Previous studies reported two distinct mechanisms for the formation of TNTs in cultured cells [14]. We utilized time-lapse microscopy to examine the formation mechanisms of TNT in HEK and C2C12 cells. The experimental results indicated that TNT formation

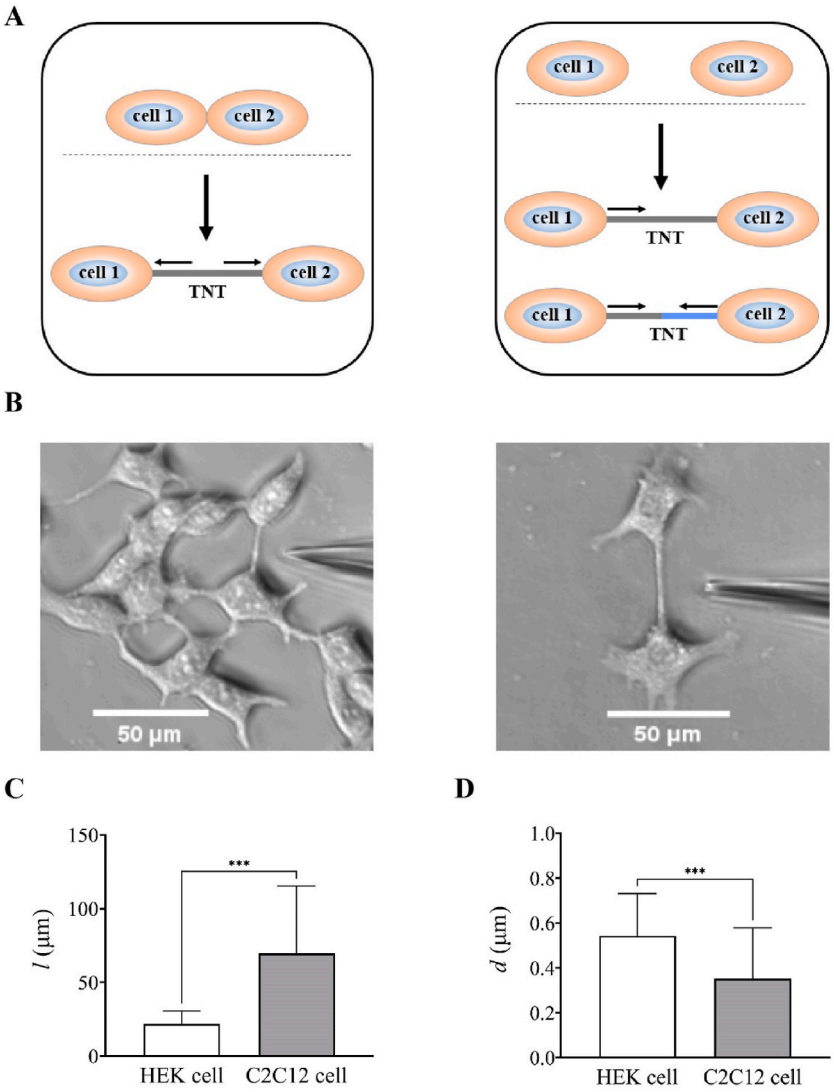

Fig. 1. Formation and geometric characteristics of TNTs in HEK and C2C12 Cells. (A) Schematic representation illustrating TNT formation in HEK and C2C12 cells. Left: TNTs were formed by cells coming into contact and then moving apart. Right: An actin-driven protrusion might connect to a neighboring cell. (B) TNT in HEK cells (left) and C2C12 cells (right). (C) The average length (*l*) of TNTs in HEK and C2C12 cells (n = 50). (D) The average diameter (*d*) of TNTs in HEK and C2C12 cells (n = 50). Significant differences are denoted with asterisks. ***P < 0.001.

in HEK cells proceeds through cell dislodgement (Fig. 1A left, movie I(A)), while the TNTs of C2C12 cells originate from the extension of continuous protrusions (Fig. 1B right, movie I(B)). Furthermore, TNTs formed by HEK cells often exhibited a network structure (Fig. 1A left), while the TNTs formed by filopodial outgrowth were mostly seen between pairs of C2C12 cells (Fig. 1A right). The average length of TNTs among HEK cells was shorter than that in C2C12 cells (Fig. 1C). The average diameter of TNTs in HEK cells was also thicker than in C2C12 cells (Fig. 1D). These results suggest that TNTs formed by the two formation mechanisms exhibit a distinct variability of diameter, length and morphology.

3.2. Effects of length and diameter on the mechanical properties of TNTs in HEK and C2C12 cells

To investigate the mechanical properties of TNTs, we used a micropipette to laterally push the midpoint of TNTs in HEK and C2C12 cells. Only straight intercellular connections (>10 μm in length) without contact with the substratum were pushed. TNTs bent when the micropipette pushed them, and immediately reassumed their original form when the push force was removed (movies II), indicating that the deformation of the TNTs was elastic. To further quantitatively analyze the elasticity of TNTs, we pushed the TNTs until eventual rupture and quantified the maximum elongation of TNTs in HEK and C2C12 cells. As shown in Fig. 2, the maximum elongations of TNTs were 1.5–2.0 in both HEK and C2C12 cells. We also found that the maximum elongations of TNTs were related to their length and diameter. Longer TNTs with a similar diameter had a smaller maximum elongation, whereas thicker TNTs with similar

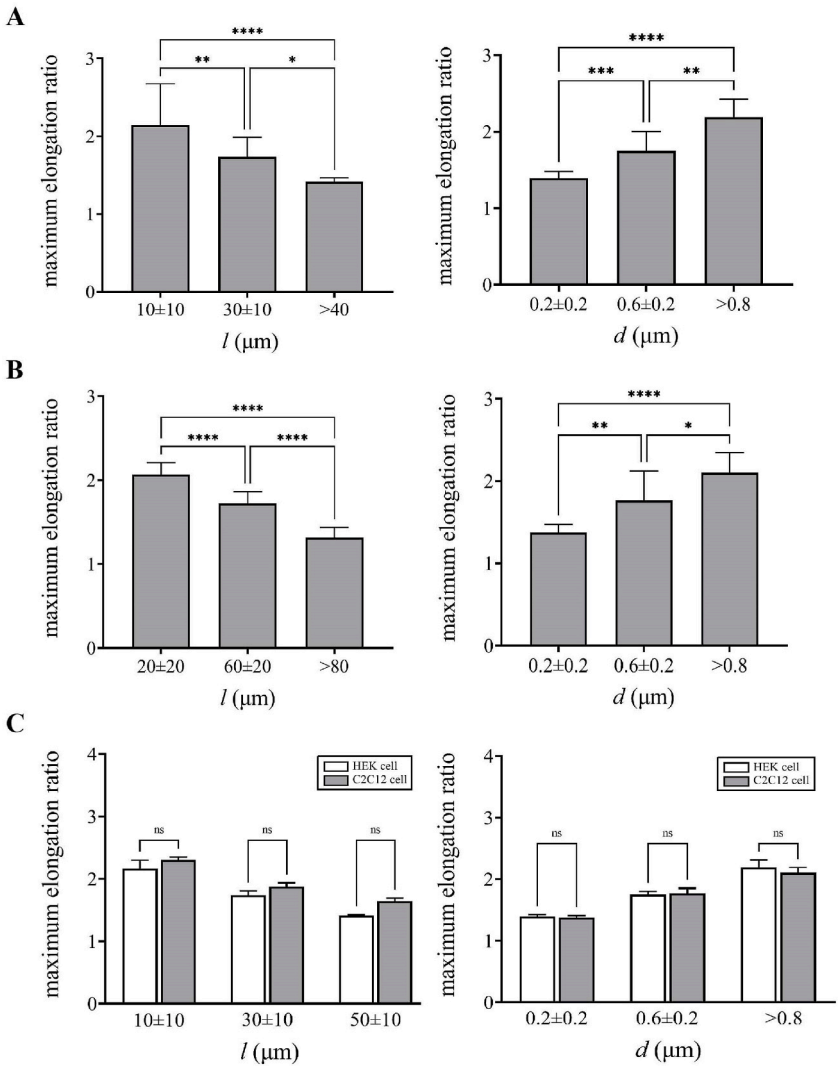

Fig. 2. Effects of length and diameter on maximum elongation of TNTs in HEK and C2C12 Cells. (A) Effects of length (*l*) and diameter (*d*) on the maximum elongation of TNTs in HEK cells (n = 48). (B) Effects of length (*l*) and diameter (*d*) on the maximum elongation of TNTs in C2C12 cells (n = 48). (C) Effects of formation mechanism on the maximum elongation of TNTs with matched length (*l*) and diameter (*d*). Significant differences are denoted with asterisks. *P < 0.05, **P < 0.01, ***P < 0.001, ****P < 0.0001.

lengths showed the opposite trend in both HKE and C2C12 cells (Fig. 2A and B). As shown in Fig. 2C, no significant difference was found in the maximum elongation of TNTs with matched diameter and matched length in both HEK and C2C12 cells. These results indicate that longer and thinner TNTs are susceptible to mechanical interference while their mechanical stability is independent of the formation mechanisms.

3.3. Effect of F-actin on the mechanical properties of TNTs

TNTs are actin-rich conduits [7]. Our cytochemical staining results demonstrated that TNT connections contained large amounts of F-actin but no tubulin in both HEK and C2C12 cells (Fig. 3A and S1). To investigate the effects of F-actin on the maximum elongation of TNTs, HEK and C2C12 cells were pre-treated with 10 μM cytochalasin D to inhibit actin polymerization. After 45 min, the TNTs were pushed with a micropipette. The results showed that the TNTs could not recover their original shape after removing the applied force in both HEK and C2C12 cells (movies III), indicating that the TNT lost their elasticity after pharmacological inhibition of actin polymerization. As shown in Fig. 3B and C, the maximum elongation of TNTs was reduced following the treatment with cytochalasin D in both cell types. However, the maximum elongation of TNTs kept the dependence on the length and diameter. Taken together, these results indicate that F-actin is essential for maintaining the elasticity and tensile strength of TNTs formed through different mechanisms.

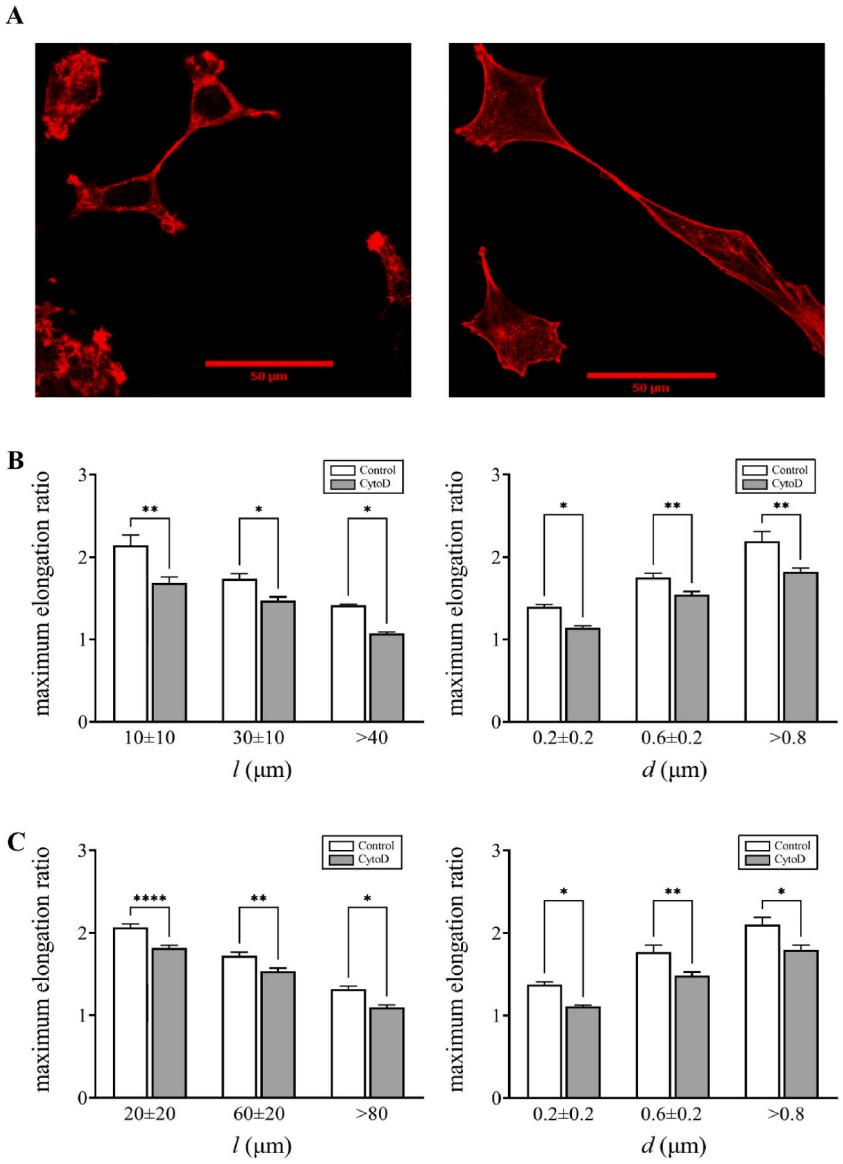

Fig. 3. Effects of F-actin on the maximum elongations of TNTs. (A) Fluorescence staining for F-actin (left: HEK cells, right: C2C12 cells). (B) Effects of inhibition of actin polymerization on the maximum elongation of TNTs with similar lengths (*l*) and diameters (*d*) in HEK cells (n = 48). (C) Effects of inhibition of actin polymerization on the maximum elongation of TNTs with similar lengths (*l*) and diameters (*d*) in C2C12 cells (n = 48). Significant differences are denoted with asterisks. *P < 0.05, **P < 0.01, ****P < 0.0001.

3.4. *Effect of extracellular Ca^{2+} between iTNTs on the mechanical properties of TNTs*

Cumulative evidence indicates that the observed intercellular links are made up of a bundle of open-ended iTNTs that are held together by N-Cadherin [8,9]. As cadherin-cadherin interactions are gated by extracellular Ca^{2+} [15], we speculated that extracellular calcium ions may affect the mechanical properties of TNTs. After the treatment with Ca^{2+}-free HBSS for 60 min, the TNTs were pushed with a micropipette. After the retraction of the push force, the TNTs immediately recover to their original form in both HEK and C2C12 cells (movies IV), indicating that TNTs still retained their elasticity without cadherin interactions. Surprisingly, Ca^{2+}-free HBSS treatment significantly increased the maximum elongation of TNTs in both HEK and C2C12 cells (Fig. 4A and B). However, the maximum elongation of TNTs in both cell types was still dependent on the length and diameter. These results suggest that the N-cadherin interactions are also critical to the mechanical properties of TNTs.

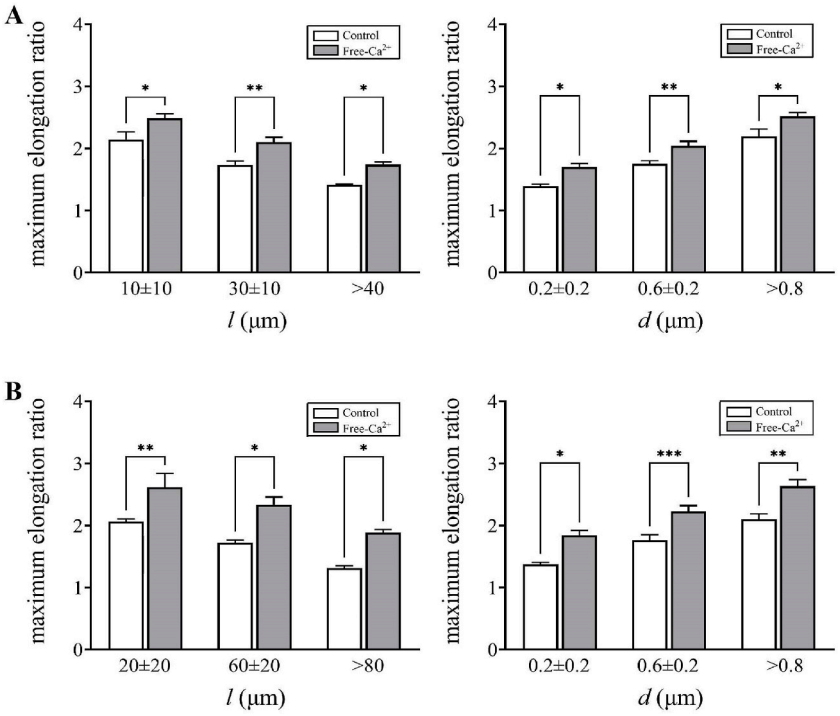

Fig. 4. Effects of extracellular Ca^{2+} on the maximum elongations of TNTs in HEK and C2C12 cells. (A) Effects of extracellular Ca^{2+} on the maximum elongation of TNTs with similar lengths (*l*) and diameters (*d*) in HEK cells (n = 48). (B) Effects of extracellular Ca^{2+} on the maximum elongation of TNTs with similar lengths (*l*) and diameters (*d*) in C2C12 cells (n = 48). Significant differences are denoted with asterisks. *P < 0.05, **P < 0.01, ***P < 0.001.

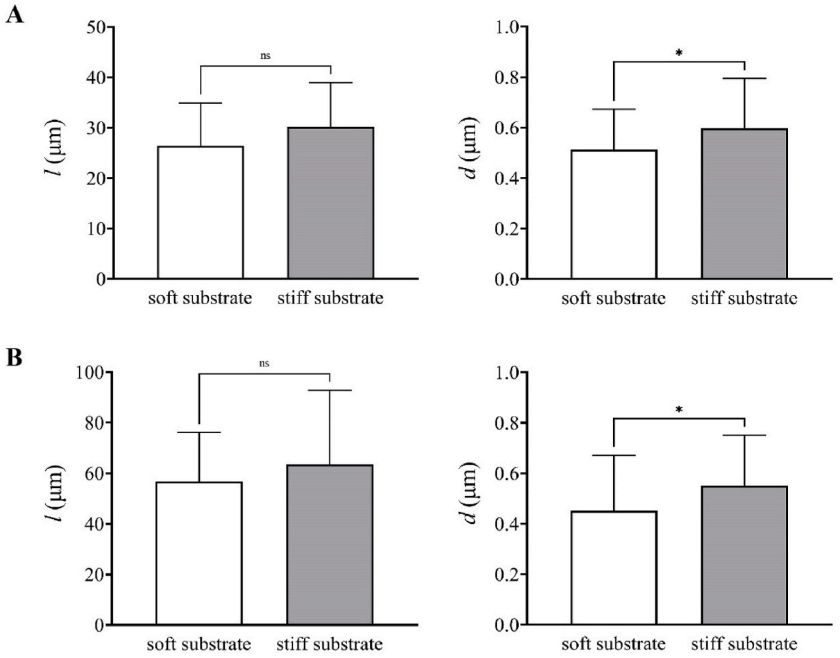

Fig. 5. Effects of ECM stiffness on the lengths and diameters of TNTs in HEK and C2C12 cells. (A) lengths (*l*) (left) and diameters (*d*) (right) of TNTs in HEK on soft and stiff substrates. (B) lengths (*l*) (left) and diameters (*d*) (right) of TNTs in C2C12 on soft and stiff substrates. Significant differences are denoted with asterisks. *P < 0.05.

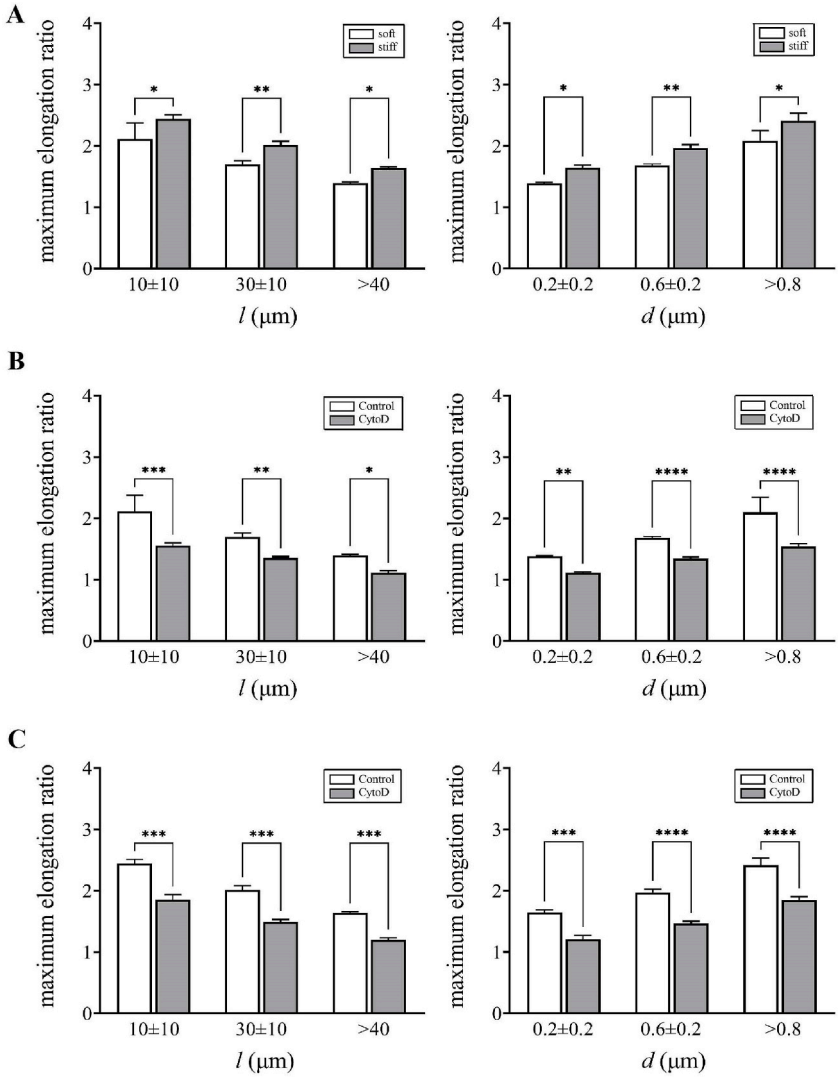

Fig. 6. Effects of ECM stiffness on the mechanical properties of TNTs in HEK cells. (A) Effects of ECM stiffness on the maximum elongation of TNTs with similar lengths (*l*) and diameters (*d*) in HEK cells (n = 48). (B) Effects of inhibition of actin polymerization on the maximum elongation of TNTs with similar lengths (*l*) and diameters (*d*) in HEK cells on soft substrate (n = 48). (C) Effects of inhibition of actin polymerization on the maximum elongation of TNTs with similar lengths (*l*) and diameters (*d*) in HEK cells on stiff substrate (n = 48). Statistically significant differences are denoted with asterisks. *P < 0.05, **P < 0.01, ***P < 0.001, ****P < 0.0001.

3.5. Effect of substrate stiffness on the formation and mechanical properties of TNTs

The formation of TNTs is influenced by many factors, including cell type, environmental conditions, and signaling molecules [16]. The extracellular matrix (ECM) is a pivotal component of various tissues and organs, acting not only as a physical scaffold for cells, but also as an orchestrator for exchanging chemical and mechanical signals [17]. Here, we explored the effect of substrate stiffness on the formation and mechanical properties of TNTs. Polyacrylamide (PA) gels have a wide range of elasticity independent of surface properties and thus are highly appropriate for studying the mechano-sensitivity of cellular processes [18]. Two types of PA-gel preparations with different stiffness were used in this study, respectively referred to as the soft (2.26kpa) and stiff (20kpa) substrates for simplicity. The diameter and length of TNTs produced by both cell types on the soft substrate were reduced compared to those produced by both cell types on the stiff substrate (Fig. 5A and B). We also found that TNTs produced by HEK and C2C12 cells on the substrates with different stiffness bent when they were pushed with a micropipette, and then immediately recovered their original form after the removal of the push force (movies V), indicating that TNTs still retain their elasticity independent of substrate stiffness. After removing the push force, the TNTs of both cell types resumed their original form more quickly on the stiff substrate (movies V(B) and (D)), indicating that the stiff substrate enhanced the elasticity of TNTs. Additionally, the maximum elongation of TNTs exhibited a diminishing trend with increasing length, while increasing with the increasing of TNT diameter in both cell types on both substrates

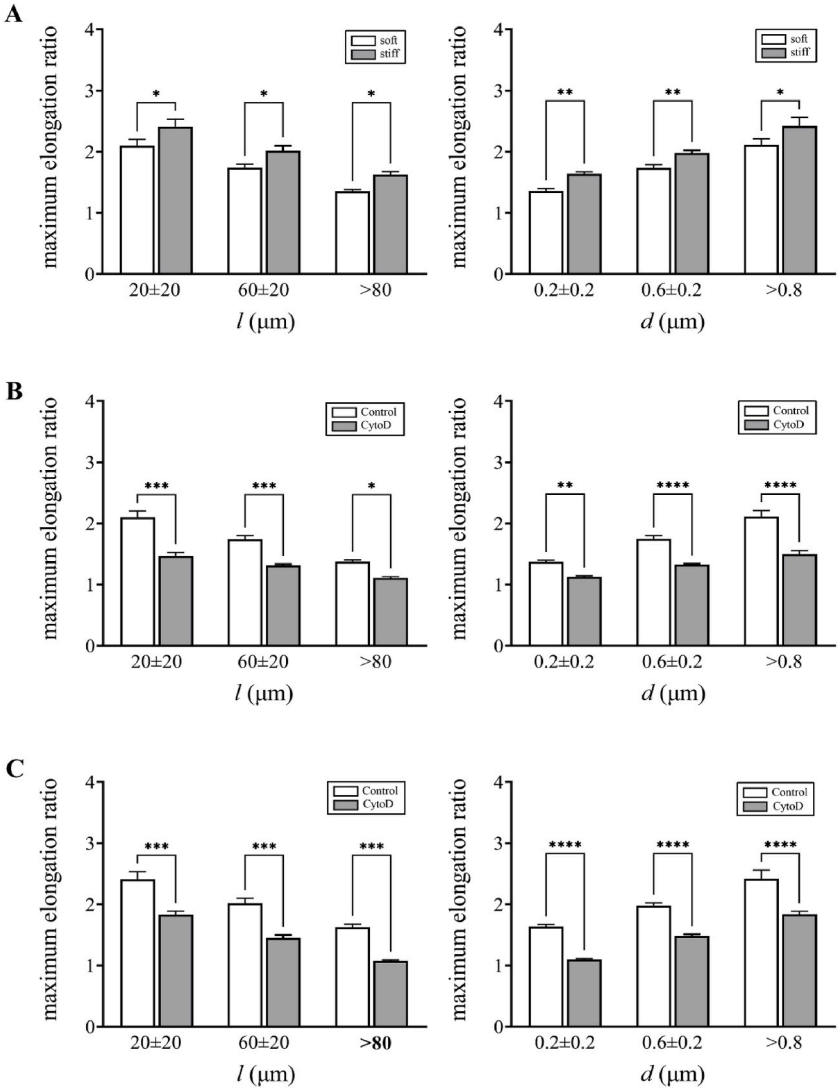

Fig. 7. Effects of ECM stiffness on the mechanical properties of TNTs in C2C12 cells. (A) Effects of ECM stiffness on the maximum elongation of TNTs with similar lengths (*l*) and diameters (*d*) in C2C12 cells (n = 48). (B) Effects of inhibition of actin polymerization on the maximum elongation of TNTs with similar lengths (*l*) and diameters (*d*) in C2C12 cells on soft substrate (n = 48). (C) Effects of inhibition of actin polymerization on the maximum elongation of TNTs with similar lengths (*l*) and diameters (*d*) in C2C12 cells on stiff substrate (n = 48). Statistically significant differences are denoted with asterisks. *P < 0.05, **P < 0.01, ***P < 0.001, ****P < 0.0001.

(Fig. 6A and 7A). The maximum elongation of TNTs with matched length or diameter ranges was greater on the stiff substrate than on the soft substrate in both cell types (Fig. 6A and 7A). After pharmacological inhibition of actin polymerization with cytochalasin D, the TNTs pushed by the micropipette could not recover their original form in either of the cell types on both substrates (movies VI), indicating that disturbing actin polymerization led to a loss of TNT elasticity. The maximum elongation of TNTs with matched length or diameter ranges was significantly reduced after the treatment with cytochalasin D on both soft and stiff substrates in both cell types (Fig. 6B, C, 7B and 7C). Taken together, these results indicate that F-actin is essential for maintaining the elasticity and tensile strength of TNTs formed by different mechanisms on both soft and stiff substrates. After applying Ca^{2+}-free HBSS to interrupt the interaction between the extracellular domains of N-cadherin molecules, the TNTs retained their original elasticity (movies VII), while the maximum elongation was significantly increased in both cell types on both substrates (Fig. 8A, B, 9A and 9B). Besides, the maximum elongation of TNTs still kept dependent on the length and diameter in both cell types on both substrates. Taken together, these results suggest that the stiff substrate could enhance the length, diameter, and maximum elongation of the TNTs formed by different mechanisms. F-actin is essential for maintaining the elasticity of TNTs, while F-actin and N-cadherin interactions of TNTs are critical for the tensile strength of TNTs in both HEK and C2C12 cells on substrates with different stiffness. We used Ca^{2+}-free HBSS to interrupt the interaction between the extracellular domains of N-cadherin molecules to explore the impact of interconnections among TNTs on the mechanical properties of TNTs.

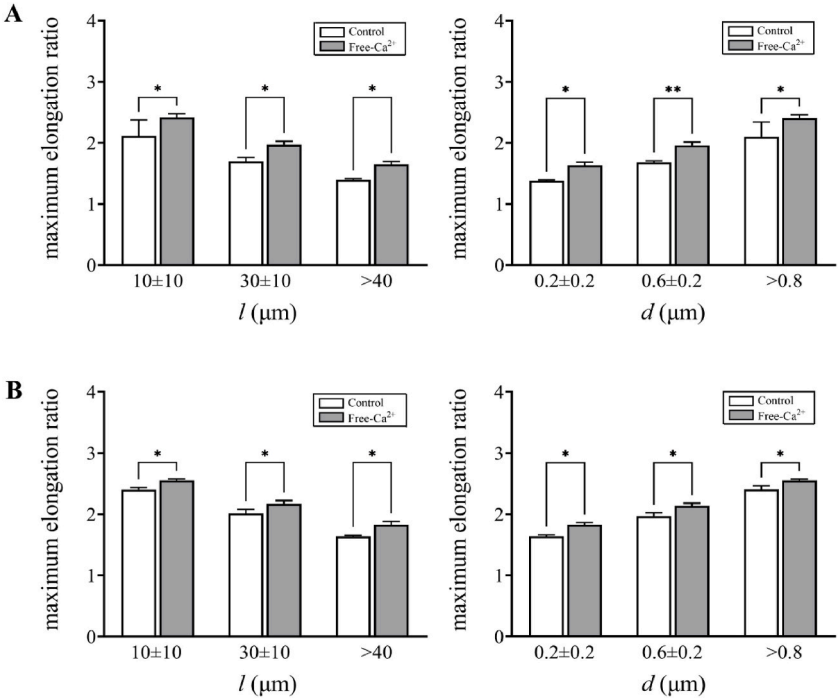

Fig. 8. Effects of connections between iTNTs on the maximum elongations of TNTs in HEK cells on soft and stiff substrates (A) Effects of iTNT connection on maximum elongation of TNTs in similar lengths (*l*) (left) and diameters (*d*) (right) in HEK cells on soft substrate (n = 48). (B) Effects of iTNT connection on maximum elongation of TNTs in similar lengths (*l*) (left) and diameters (*d*) (right) in HEK cells on stiff substrate (n = 48). Significant differences are denoted with asterisks. *P < 0.05, **P < 0.01.

4. An elastic model of TNTs

To deepen our understanding of the experimental findings described above (Fig. 10B), we established a theoretical model by considering the TNT as a beam with fixed supports at its two ends, A and B. The beam is loaded by the force **F** at its midpoint. The initial length of the beam is designated as *l*. The cross-section of TNT is circular, with the diameter *d*, and its bending stiffness is represented as *EI*, where *E* is the elastic modulus of TNT and *I* is the polar moment of inertia of TNT. We cut through the beam at a cross-section located at the distance *x* from its left end and isolate the left-hand part of the beam as a free body (Fig. 10C). The free body is in equilibrium by the force $\mathbf{F}_A$, bending moment $\mathbf{M}_A$ and the shear force **P** that act over the cut cross-section. The structure of TNT is made up of a few iTNTs (Fig. 10A), which are connected by N-Cadherin [8]. *n* is iTNT number that can significantly influence the TNT mechanical properties, such as elasticity and stability.

Each iTNT contains multiple parallel actin filaments that are held together by actin-binding protein (ABP) [19] (Fig. 10A). The distance between two adjacent filaments is 12.26 nm [20]. Therefore, we can estimate that a TNT contains 815 actin filaments when its diameter is 0.35 μm. The TNT contains 8 iTNTs and each iTNT contains 101 actin filaments. In this case, each iTNT has the same bending stiffness. In Fig. 11, we observe that the deflection calculated from the infinitesimal theory is the same as that calculated from the commercial software Abaqus. In the theoretical model, the force $\mathbf{F}_A$ corresponds to the force at a specific moment during the loading process. While maintaining a concentrated force constant, it becomes evident that the deflection at the midpoint of the TNT grows in proportion to the length of the TNT. Furthermore, within a specific length of TNT, the deflection at the midpoint increases as the concentrated force rises. It is noteworthy that when the deflection at the midpoint exceeds 5 % of the TNT length, the utilization of the large deformation theory for beam analysis becomes imperative to ensure accurate resolution.

As we change the diameter of TNT within the range of 0.1 μm to 1 μm, the number of actin filaments of TNT increases, as depicted in Fig. 12A. Consequently, this increase in actin filaments results in an augmentation of the bending stiffness of TNT, as illustrated in Fig. 12B. As the bending stiffness of TNT increases, the maximum elongation of TNT also rises. These findings are consistent with the results obtained in our experiments, as detailed in Fig. 2A and B. When maintaining a constant diameter of TNT, we employ a Ca^{2+}-free HBSS solution to disrupt the interaction between iTNTs. This resulted in iTNT fusion and a decrease in the number of iTNTs, consequently leading to an increase in the diameter of each iTNT. Therefore, their bending stiffness is enhanced, as depicted in Fig. 12B. This enhanced bending stiffness is associated with a greater maximum elongation when TNT is subjected to micropipette-induced force.

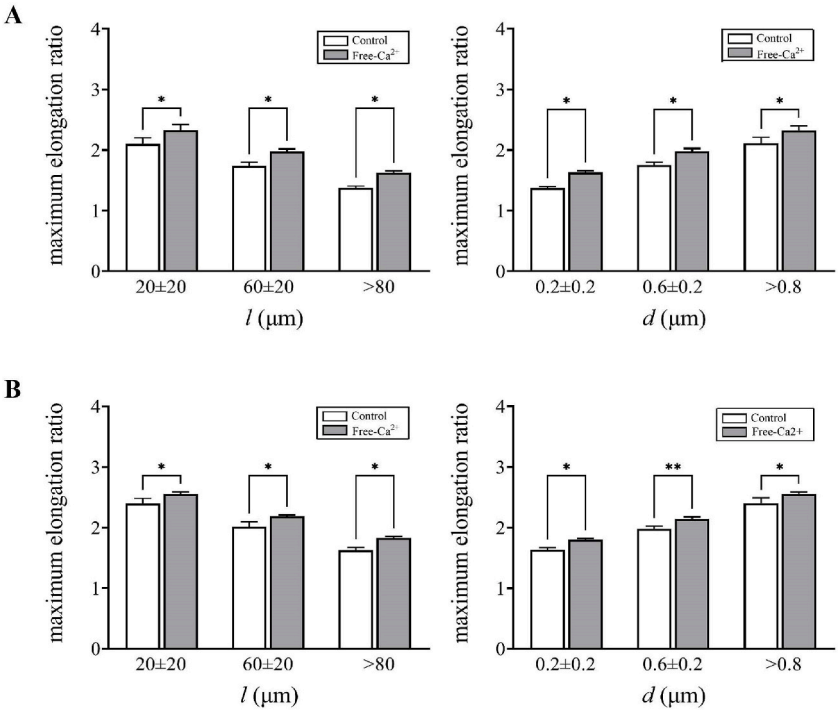

Fig. 9. Effects of connections between iTNTs on the maximum elongations of TNTs in C2C12 cells on soft and stiff substrates (A) Effects connections between of iTNT on maximum elongation of TNTs with similar lengths (*l*) (left) and diameters (*d*) (right) in C2C12 cells on soft substrate (n = 48). (B) Effects connections between of iTNT on the maximum elongation of TNTs with similar lengths (*l*) (left) and diameters (*d*) (right) in C2C12 cells on stiff substrate (n = 48). Significant differences are denoted with asterisks. *P < 0.05, **P < 0.01.

5. Discussions

About twenty years ago, TNTs were discovered as a new mode of intercellular communication between animal cells [3]. Subsequent investigations have confirmed the presence of intercellular TNTs in various cell types, including immune cells, astrocytes, neurons, and tumor cells [4,5]. These unique structures facilitate the long-range transport of diverse cargoes, encompassing viruses, organelles such as lysosomes, as well as Ca^{2+} and electrical signals [4,5,21]. The transport efficiency of TNTs is largely dependent on their number, which in turn is determined by the formation and stability of TNTs. Cells and subcellular compartments are often subjected to mechanical effects during physiological processes [22]. When subjected to mechanical loading, the number of TNTs is dependent on their mechanical stability. Although the mechanical properties of TNTs have been tested using atomic force microscopy and optical tweezers [9,12], these tools could only cause small deformations of TNTs, and failed to accurately measure the mechanical properties under large deformation, such as elasticity and maximum elongation. To overcome these limitations, we here designed a new mechanical loading method that can cause large deformation of TNTs. In this method, the midpoint of TNT is pushed using a fire-polished glass pipette mounted on a micromanipulator, which can cause deformations of different magnitudes. We believe it can more accurately determine the mechanical properties and stability of TNTs.

It is widely recognized that TNTs can be formed by two mechanisms: the protrusion driven by the polymerization of actin (type-I), and the dislodgement of adjacent cells, which draw out nanotubes when they move apart (type-II) [7]. In this paper, we report for the first time that type-I TNTs (C2C12 cell) are longer in length but smaller in diameter than type-II TNTs (HEK cells; Fig. 1C and D). One possible reason for this difference is that the two types of TNTs are formed by different driving forces. However, the two types of TNTs share similar elastic structures, and the maintenance of TNT elasticity requires normal F-actin polymerization. This indicates that the elasticity of TNTs depends on the tension of the cytoskeleton, and the membrane tension alone is insufficient to maintain the elasticity of TNTs. More importantly, our study demonstrates that the maximum elongation is related to the length and diameter of both type-I and II TNTs (Fig. 2). This is different from a previous report [9], which indicated that the maximum elongation did not show a significant correlation with the length of TNTs. These contradictory results may be attributed to different testing methods.

Consistent with a previous report [7], our immunofluorescence imaging showed that type-I and II TNTs are actin-rich conduits (Fig. 3A). Thus, we hypothesized that upon diameter increase, the thicker TNTs provided a larger space for the precursors needed for actin polymerization, resulting in greater maximum elongation. After pharmacological inhibition of actin polymerization, the maximum elongation of TNTs was significantly reduced in both HEK and C2C12 cells (Fig. 3B and C). We therefore concluded that F-actin is essential for the mechanical stability of TNTs. Furthermore, the membrane tension of long TNTs is higher than that of short TNTs [10]. Many cell types store an excess of membrane material [23], and the membrane reservoir of TNTs decreases with increasing

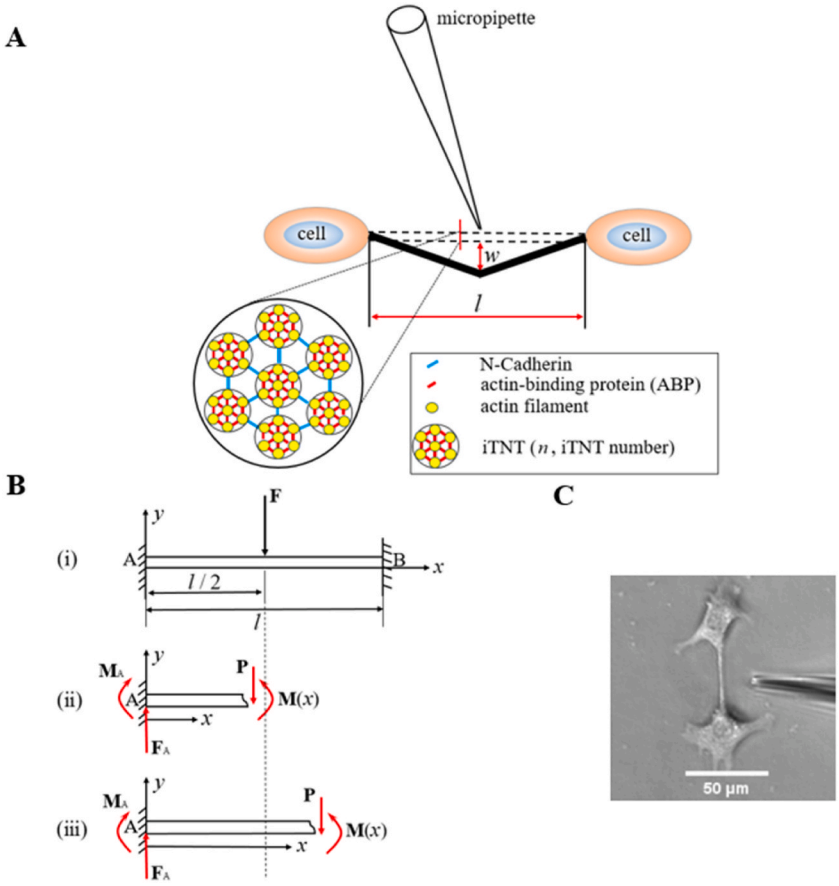

Fig. 10. Schematic diagram of manipulating TNT. (A) Schematic representation illustrating the process of pushing TNT by a micropipette. (B) Bright-field image of pushing TNT by a micropipette. (C) Shear force **P** and bending moment **M**(x) in the beam.

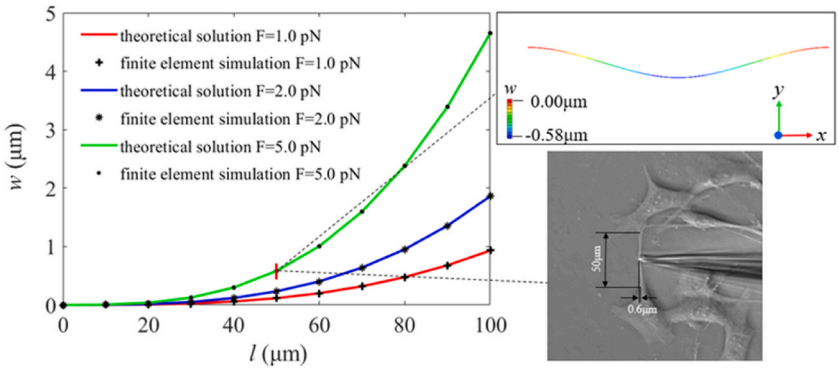

Fig. 11. The deformed configuration of the beam with F = 1 pN, 2 pN and 5 pN.

membrane tension, which may explain the decrease in the maximum elongation of longer TNTs. Taken together, our results suggest that the maximum elongation of long and thin TNTs is decreased due to a low F-actin content and smaller membrane reservoir, while the increased maximum elongation of short and thick TNTs is largely due to high F-actin content and larger membrane reservoir. TNTs made up of several iTNTs held together by N-Cadherin were found recently in many cell types. This conformation might greatly increase their stability and elasticity, allowing them to withstand movements between connected cells [9,10]. Surprisingly, after interrupting the interaction of extracellular domains of N-cadherin molecules between iTNTs, the maximum elongation increased significantly (Fig. 4A and B). These results were contrary to previous hypotheses [9,10]. In addition, it was recently shown that individual membrane tubes fused to form thicker extensions after treatment with low concentrations of trypsin [24]. We therefore

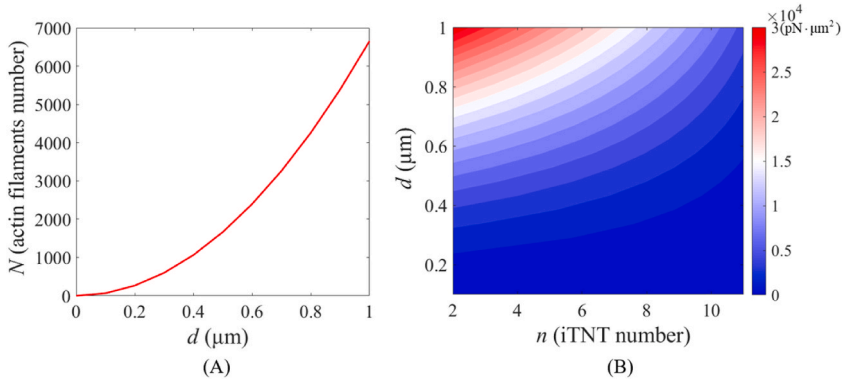

Fig. 12. The actin filaments number and the bending stiffness with varying *d* **(the diameter of TNT).** (A) The actin filaments number versus varying *d* (the diameter of TNT). (B) The bending stiffness versus varying *d* (the diameter of TNT) and *n* (iTNT number).

speculate that iTNTs fused to form thicker TNT extensions after treatment with Ca^{2+}-free HBSS. The tube formed by the fusion of iTNTs may provide space for the synthesis or entry of microtubules, which enhances its tensile strength. However, interrupting the interaction of extracellular domains of N-cadherin molecules between iTNTs resulted in increased maximum elongation of TNTs, and the underlying mechanism needs further investigation.

ECM stiffness affects a wide range of cellular behaviors such as proliferation, differentiation, apoptosis, organization, or migration and has thus been intensively studied in recent years [22]. In this study, we found that the stiff substrate could increase the length, diameter and maximum elongation of TNTs formed by both HKE and C2C12 cells (Fig. 5). This effect can be partly attributed to the fact that increased ECM stiffness-induced changes of the actin-cytoskeletal content and membrane reservoir, which may enhanced the mechanical stability of TNTs. The effects of both F-actin and N-Cadherin on the mechanical properties of TNTs showed the same trend in HEK and C2C12 cells on substrates with different stiffness (Fig. 6B, C, 7B, 7C,8, and 9).

In conclusion, we have established an accurate method to measure the mechanical properties of TNTs. This work explored the factors that affect the mechanical properties of TNTs in terms of their lengths, diameters, cytoskeleton components, N-cadherin molecules and formation mechanisms. These findings not only deepen the understanding of TNTs and related dynamics behaviors of cells, but also may provide new clues for drug development targeting TNTs also.

CRediT authorship contribution statement

Yanli Sun: Writing – original draft, Methodology, Data curation, Conceptualization. **Huikai Zhang:** Methodology, Investigation, Data curation. **Ilya B. Zavodnik:** Methodology. **Hucheng Zhao:** Writing – review & editing, Supervision, Funding acquisition. **Xiqiao Feng:** Writing – review & editing, Supervision, Funding acquisition.

Declaration of competing interest

The authors declare that they have no known competing financial interests or personal relationships that could have appeared to influence the work reported in this paper.

Acknowledgments

The authors acknowledge the support from the National Natural Science Foundation of China (Grant Nos. 12072176, 12211530450, 12032014 and 11921002).

Appendix A. Supplementary data

Supplementary data to this article can be found online at https://doi.org/10.1016/j.heliyon.2024.e36265.

References

[1] S. Sowinski, D.M. Davis, Membrane nanotubes: dynamic long-distance connections between animal cells, Nat. Rev. Mol. Cell Biol. 9 (2008) 431–436.
[2] D. Cordero Cervantes, C. Zurzolo, Peering into tunneling nanotubes—the path forward, EMBO J. 40 (8) (2021).
[3] A. Rustom, R. Saffrich, I. Markovic, et al., Nanotubular highways for intercellular organelle transport, Science 303 (2004) 1007–1010.
[4] R. Chakraborty, T. Nonaka, M. Hasegawa, et al., Tunnelling nanotubes between neuronal and microglial cells allow bi-directional transfer of α-Synuclein and mitochondria, Cell Death Dis. 14 (5) (2023).

[5] A. Chauveau, A. Aucher, P. Eissmann, et al., Membrane nanotubes facilitate long-distance interactions between natural killer cells and target cells, Proc. Natl. Acad. Sci. U.S.A. 107 (2010) 5545–5550.
[6] C. Zhang, R. Schekman, Syncytin-mediated open-ended membrane tubular connections facilitate the intercellular transfer of cargos including Cas9 protein, Elife 12 (2023) e84391.
[7] O. Korenkova, A. Pepe, C. Zurzolo, Fine intercellular connections in development: TNTs, cytonemes, or intercellular bridges? Cell Stress 4 (2020) 30–43.
[8] A. Sartori-Rupp, D. Cordero Cervantes, A. Pepe, et al., Correlative cryo-electron microscopy reveals the structure of TNTs in neuronal cells, Nat. Commun. 10 (2019), https://doi.org/10.1038/s41467-018-08178-7.
[9] A. Li, X. Han, L. Deng, et al., Mechanical properties of tunneling nanotube and its mechanical stability in human embryonic kidney cells, Front. Cell Dev. Biol. 10 (2022), https://doi.org/10.3389/fcell.2022.955676.
[10] M. Drab, D. Stopar, V. Kralj-Iglič, et al., Inception mechanisms of tunneling nanotubes, Cells 8 (6) (2019) 626.
[11] R. Polak, B.D. Rooij, R. Pieters, et al., B-cell precursor acute lymphoblastic leukemia cells use tunneling nanotubes to orchestrate their microenvironment, Blood 126 (21) (2015) 2404–2414.
[12] M. Chang, O.C. Lee, G. Bu, et al., Formation of cellular close-ended tunneling nanotubes through mechanical deformation, Sci. Adv. 8 (13) (2022).
[13] S. Patwardhan, P. Mahadik, O. Shetty, et al., ECM stiffness-tuned exosomes drive breast cancer motility through thrombospondin-1, Biomaterials 279 (2021) 121185.
[14] A. Rustom, Hen or egg? Some thoughts on tunneling nanotubes, Annals of the New York Academy of Sciences 1178 (1) (2009) 129–136.
[15] S.A. Kim, C.-Y. Tai, L.-P. Mok, et al., Calcium-dependent dynamics of cadherin interactions at cell–cell junctions, Proc. Natl. Acad. Sci. USA 108 (24) (2011) 9857–9862.
[16] R. Mittal, E. Karhu, J.S. Wang, et al., Cell communication by tunneling nanotubes: implications in disease and therapeutic applications, J. Cell. Physiol. 234 (2019) 1130–1146.
[17] Sergeyv, Plotnikov, et al., Force fluctuations within focal adhesions mediate ECM-rigidity sensing to guide directed cell migration - ScienceDirect, Cell 151 (7) (2012) 1513–1527.
[18] J.R. Tse, A.J. Engler, Preparation of hydrogel substrates with tunable mechanical properties, Curr. Protoc. Cell Biol. 47 (1) (2010).
[19] B.A.T.H.E. Mark, et al., Cytoskeletal bundle mechanics, Biophys. J. 94 (8) (2008) 2955–2964.
[20] S. Aramaki, K. Mayanagi, M. Jin, et al., Filopodia formation by crosslinking of F-actin with fascin in two different binding manners, Cytoskeleton 73 (7) (2016) 365–374.
[21] C. Zurzolo, Connections that couple brain activity to blood flow, Nature 585 (2020) 32–33.
[22] L. Pasakarnis, D. Dreher, D. Brunner, SnapShot: mechanical forces in development I, Cell 165 (3) (2016) 754.
[23] B. Sinha, D. KöSTER, R. Ruez, et al., Cells respond to mechanical stress by rapid disassembly of caveolae, Cell 144 (3) (2011) 402–413.
[24] O. Staufer, A. Rustom, Protease-resistant cell meshworks: an indication of membrane nanotube-based syncytia formation, Exp. Cell Res. 372 (2) (2018) 85–91.